

the symmetry and the phonon normal modes in the multi-layered graphene

Jin-Wu Jiang,^{1,*} Bing-Shen Wang,² and Zhao-Bin Su^{1,3}

¹*Institute of Theoretical Physics, Chinese Academy of Sciences, Beijing 100080, China*

²*State Key Laboratory of Semiconductor Superlattice and Microstructure*

and Institute of Semiconductor, Chinese Academy of Sciences, Beijing 100083, China

³*Center for Advanced Study, Tsinghua University, Beijing 100084, China*

(Dated: June 21, 2024)

The symmetry groups of the N -stacked of graphene layers (NSGL's) structure with even and odd N are identified respectively. The corresponding phonon modes and the infra-red and Raman active properties are analyzed. The dispersions of various mode are calculated mainly for the 2 or 3-layer stacked graphene structure. In particular, there is a exotic normal mode in the NSGL's whether it is Raman active or not depends the even-oddness of N , this could be very useful in determining experimentally whether N is even or odd .

PACS numbers: 81.05.Uw, 63.22.+m

In recent years, the ultrathin graphite films which is N (> 1) stacked of graphene layers (NSGL's) are successfully fabricated the experimentally¹. Since the NSGL's are regarded as the competitive candidates for the design of novel nano-devices, extensive studies have been devoted to these systems. To figure out their symmetry properties, analyzing corresponding electron and phonon spectrum, relevant selection rules and the optical activities should be fundamental and interesting. However, to our knowledge, although there are some studies on electronic structure², no works concerning either the symmetry analyse or the phonon normal modes for the NSGL's exists.

In this paper, we will show that the symmetry groups for NSGL's with N (> 1) even (ENSGL's) and odd (ON-SGL's) are D_{3d} and D_{3h} respectively. We further classify the phonon normal modes at Γ point and determine the Raman and Infra-red (Ir) active modes of the NSGL's. In particular, there is an interesting normal mode which is Raman active in the ENSGL's while inactive in ON-SGL's. This mode can be useful in determining whether the number N for the NSGL's is even or odd experimentally. Moreover, we generalize the force constant model of graphene³ into NSGL's and calculate the phonon dispersions for the 2- and 3-layered graphene. Frequencies for the Raman and Ir active modes are predicted. We also show that there is a significant difference in the low-frequency region between the 2-layered graphene and the 3-dimensional (3D) graphite.

Graphene is a single layer of carbon atoms with the honeycomb lattice configuration which is characterized by the D_{6h} symmetry⁴, and corresponding 2D group is C_{6v} . The 3D graphite is AB-stacked honeycomb lattice, the B layers are achieved by shifting the A layers along one of its first-nearest carbon-carbon bonds in the horizontal plane as shown in Fig. 1. The space group of the 3D graphite is non-symmorphic group D_{6h}^4 with non-primitive translation $\vec{\tau} = \frac{1}{2}\vec{c}$ (primitive translation $\vec{t} = n_1\vec{a}_1 + n_2\vec{a}_2 + n_3\vec{c}$).⁵ The distance between two adjacent layers is about $\frac{c}{2} = 3.35\text{\AA}$ which is much larger than the bond length between two nearest-neighbor atoms

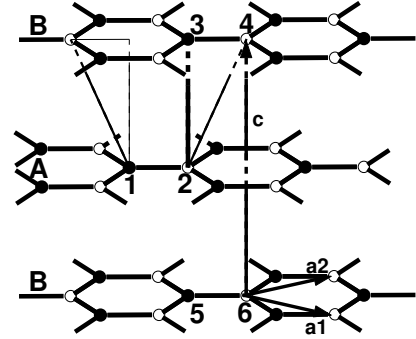


FIG. 1: The sketch of the configuration for the stacked graphene layers.

in the plane, $b = 1.42\text{\AA}$. The NSGL's are also constructed by AB-stacked honeycomb lattice, but with limited layers. Although the structure of each layer of 3D graphite and ENSGL's are same, the corresponding symmetry group are different since the displacement symmetry along \vec{c} axis no longer exists, so does the symmetry associated with $\vec{\tau}$. Now the symmetry group becomes a direct product of a 3D point group and a 2D translational group. And the point group is different for ENSGL's and ON-SGL's.

For the ENSGL's, a center of inversion σ_i occurs in the middle of atoms 2 in the $\frac{N}{2}$ -th layer and 3 in the $\frac{N}{2} + 1$ -th layer as shown in Fig. 1. There are one 3-fold main axis in the direction perpendicular to the layers and three 2-fold axes, C_2'' , perpendicular to the main axis at angles of $\pi/3$ to each other. All these symmetry operations together constitute the point group $D_{3d} = \{E, 3C_3, 3C_2''\} \times \{E, \sigma_i\}$.

In the ON-SGL's, instead of the center of inversion there is a reflection symmetry σ_h with the middle layer as its reference plane. A 3-fold main axis exists in the direction of z -axis and three 2-fold axes, C_2' , are perpendicular to it. We notice that these three 2-fold axes C_2' are one

to one perpendicular to those of C_2'' . Consequently, the symmetry group for the odd number of stacked graphene layers is $D_{3h} = \{E, 3C_3, 3C_2'\} \times \{E, \sigma_h\}$.

The environment of an atom in the graphite and NSGL's is different from that in 2D graphene. For each carbon atom in the graphene layer, there are three nearest-neighbor carbon atoms and six next-nearest-neighbors. There are four carbon atoms 1, 2, 3, 4 in a unit cell of graphite, as represented in Fig. 1. For atom 2 in the A layer, there are two inter-layer nearest-neighbors in each of the two adjacent layers, with the distance c . Also, in each of the two adjacent layers, there are three inter-layer next-nearest-neighbor atoms around atom 2 with distance $\sqrt{b^2 + c^2}$. As illustrated in Fig. 1, the adjacent environment for atom 1 is quite different from that of atom 2. It has no inter-layer first-neighbors with the same distance as c . However, atom 1 has six inter-layer neighbors in each of the two adjacent layers with the same distance as that of the second-nearest-neighbor of atom 2.

The dynamical representation $\Gamma^{dyn} = \Gamma^v \otimes \Gamma^{atom}$ can be decomposed into the irreducible representations of the symmetry group, with the lattice displacements as the bases, where Γ^v is the vector representation and Γ^{atom} is the permutation representation of the group. By applying the projection operator technique, we carry out the decomposition of the dynamical representation into the irreducible representations for the four systems: the single graphene layer, the graphite, ENSGL's and ONSGL's. Following Elliott⁶, the infra-red(Ir) active phonon modes belongs to the irreducible representations decomposed from the vector representation Γ^v , while the Raman active modes correspond to the irreducible representations shown up in the decomposition of a six dimensional representation with bases as the quadratic forms: $x^2 + y^2$, z^2 , $x^2 - y^2$, xy , yz , and zx . The three acoustic modes with zero frequency at the Γ point, which correspond to the vector representation Γ^v , are excluded in the consideration of Ir and Raman active modes. We now determine the Ir and Raman active modes. The symbol for the irreducible representations we used here is the notation used in Ref. 7 which is most commonly used in the treatment of molecules.

The phonon modes of single layer graphene at Γ should have the point group D_{6h} symmetry⁴. There are six normal modes, in which three are zero frequency acoustic modes and two are Raman active in-plane optical modes.

$$\Gamma^{dyn} = A_{2u} \oplus B_{2g} \oplus E_{1u} \oplus E_{2g}, \quad \Gamma^R = E_{2g}, \quad (1)$$

where the Γ^R denotes the Raman active modes. There is no Ir active modes.

The space group for the graphite is known as D_{6h}^4 . The 12 phonon modes at Γ point can be classified by the following irreducible representations.⁸ The irreducible representations of the Ir and Raman active modes can be read off from Γ^{Ir} and Γ^R respectively.

$$\Gamma^{dyn} = 2(A_{2u} \oplus B_{2g} \oplus E_{1u} \oplus E_{2g}), \quad (2)$$

$$\Gamma^{IR} = A_{2u} \oplus E_{1u}, \quad \Gamma^R = 2E_{2g}. \quad (3)$$

As analyzed above, the symmetry group of the ENSGL's is D_{3d} . There are $6N$ phonon modes at Γ point which can be classified by the following irreducible representations.

$$\Gamma^{dyn} = N(A_{1g} \oplus A_{2u} \oplus E_g \oplus E_u), \quad (4)$$

$$\Gamma^{IR} = (N-1)A_{2u} \oplus (N-1)E_u, \quad (5)$$

$$\Gamma^R = NA_{1g} \oplus NE_g. \quad (6)$$

For ONSGL's, the symmetry group is D_{3h} , and the $6N$ phonon modes at Γ point correspond to the following irreducible representations in Γ^{dyn} , and those of the Ir as well as Raman active modes are further assembled as

$$\Gamma^{dyn} = (N-1)A_1' \oplus (N+1)A_2'' \oplus (N+1)E' \oplus (N-1)E'', \quad (7)$$

$$\Gamma^{IR} = NA_2'' \oplus NE', \quad (8)$$

$$\Gamma^R = (N-1)A_1' \oplus NE' \oplus (N-1)E''. \quad (9)$$

Since the σ_i symmetry and σ_h symmetry can not co-exist in the ENSGL's and ONSGL's, we can see two straightforward consequences from the above classification for the Ir and Raman active modes. Firstly, in the ENSGL's, phonon modes can not be Ir and Raman active simultaneously (which is also true for the graphene and graphite). However, in the ONSGL's, the N E' modes are both IR and Raman active. This is because there is no inversion center in the ONSGL's.

Secondly, among the optical modes with their vibrational displacements perpendicular to the constituent layers, there is an exotic mode oscillating with each layer as a whole but alternatively from layer to layer. It belongs to the A_{1g} in the ENSGL's and A_2'' in the ONSGL's. Since the σ_h operation exists only in the ONSGL's, this mode is Raman active in the ENSGL's while it is inactive in the ONSGL's. Nevertheless, its vibrational mode favors to take the maximum advantage of the inter-layer interactions, it would be sensitive and useful experimentally to identify the even-oddness of the NSGL's with a few of layers.

The vibrational potential energy for a graphene sheet can be described by five quadratic terms with five force constant.³ They are the 1st and 2nd nearest-neighbor stretching, the in-plane bond angle variations, the out-of-surface bond bending and the bond twisting vibrational potential energy. Here we generalize this model to include the vibrational energy with regard to the inter-layer interaction. As shown in Fig. 1, there is only one inter-layer nearest-neighbor carbon-carbon bond in each unit cell (the bond between atoms 2 and 3) and there is no bond angle formed by two inter-layer nearest-neighbor bonds. Henceforth, the two energy terms associate with the bond angle variation both in-plane and out-of-plane

TABLE I: Comparison of several mode frequencies (in the unit of cm^{-1}) between the calculated results (following our model) and the experimental values.¹¹

Reps	E_{2g}	B_{2g}	A_{2u}
experiments ¹¹	40	127	868
our theory	38	135	871

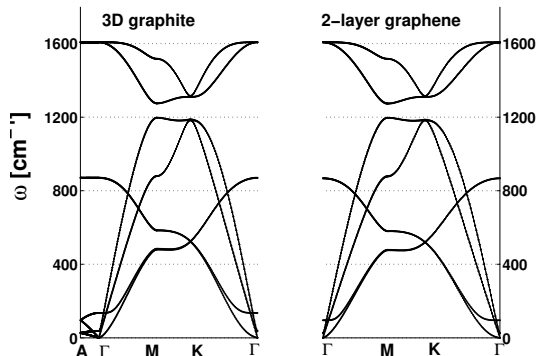


FIG. 2: (a). The phonon dispersion along some high-symmetry directions for the 3D graphite. (b). The dispersion for 2-layer stacked graphene. The significant differences between (a) and (b) is in the low-frequency region as shown in Fig. 5.

need not to be accounted for the inter-layer vibrational potential energy. Only the remaining three energy terms have to be considered for the inter-layer interaction as illustrated in the following.

(1). The inter-layer bond stretching energy $V_l^{(int)}(V_{sl}^{(int)})$ has the form as:

$$\sum_{i,j} \frac{\hat{k}_l}{2} [(\vec{u}_i - \vec{u}_j) \cdot \vec{e}_{ij}^d]^2, \quad (10)$$

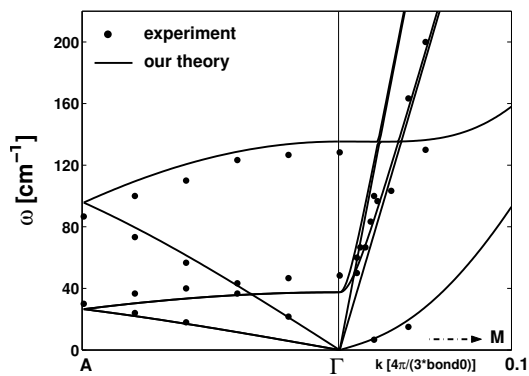


FIG. 3: Phonon dispersion for the 3D graphite in the low-frequency region. Solid dots are the experimental results in Ref. 11. Our theoretical calculations are shown in lines.

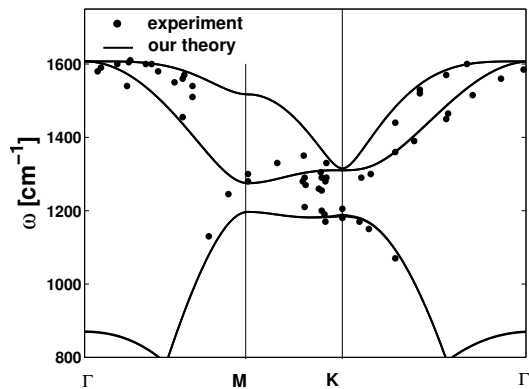


FIG. 4: Phonon dispersion for the 3D graphite in the high-frequency region. Solid dots are the experimental results.¹² In Ref. 12, those phonon wave vectors \vec{q} , which were not exactly along the Γ -M or Γ -K-M direction, were projected onto the closest high-symmetry direction. Lines are our theoretical calculations.

where $\vec{u}_i(\vec{u}_j)$ is the displacement vector of the atom $i(j)$ and \vec{e}_{ij}^d is the unit vector from atom i to atom j . If the summation is taken over the nearest-neighbored inter-layer pair of atoms, the corresponding force constant is denoted as \hat{k}_l while for next nearest-neighbor inter-layer pairs we have the force constant as \hat{k}_{sl} .

(2). As shown in Fig. 1, for each pair of inter-layer carbon atoms 2 and 3, each of which is associate with three intra-layer first-nearest-neighbors, the twisting potential energy for this bond can be described in the following forms.

$$V_{tw} = \frac{\hat{k}_{tw}}{2} \left[\sum_i (\vec{u}_i - \vec{u}_2) \cdot \vec{e}_i^\theta - \sum_j (\vec{u}_j - \vec{u}_3) \cdot \vec{e}_j^\theta \right]^2, \quad (11)$$

where \sum_i and \sum_j represent the summation over the three intra-plane first-nearest-neighbors for atoms 2 and 3 respectively. $\vec{e}_i^\theta = \vec{e}_z \times \vec{e}_{2i}^d$ is the tangential unit vector in the plane for the bond between atoms 2 and i . Furthermore, the expression in the quadratic form as a whole is actually a proper definition for the torsion angle for the bond between atoms 2 and 3. For pure rotations around the bond, this expression gives zero torsion consistently. Nevertheless, the bond between atoms 2 and 3 is most severely twisted when the three neighbors around atom 2 and that of atom 3 rotate reversely.

We stress here that, all of the above three inter-layer vibrational potential energy terms satisfy the rigid translational and rotational symmetry requirements⁹. They also guarantee the existence of the flexure modes in the four systems, which are characteristic of the system with lowering dimensions such as plate and surface.

The five intra-layer force constants we used in the following have been settled down in Ref. 10. We further adjust the three inter-layer force constants to fit the experimental values of three specified low frequency modes in

TABLE II: The Raman and IR mode frequencies (in the unit of cm^{-1}) for the 3D graphite, 2-layer and 3-layer stacked graphene are listed in the 1st, 2nd and 3rd line. The irreducible representations are presented in the brackets following the frequency value.

	Raman		Infra-red	
3D	37.5 (E_{2g})	1607.1 (E_{2g})	870.8 (A_{2u})	1607.3 (E_{1u})
2-layer	26.5 (E_g)	95.7 (A_{1g})	867.8 (A_{2u})	1607.1 (E_u)
	867.1 (A_{1g})	1607.0 (E_g)		
3-layer	18.7 (E'')	32.5 (E')	32.5 (E')	117.2 (A_2'')
	67.7 (A_1')	867.4 (A_1')	867.3 (A_2'')	870.2 (A_2'')

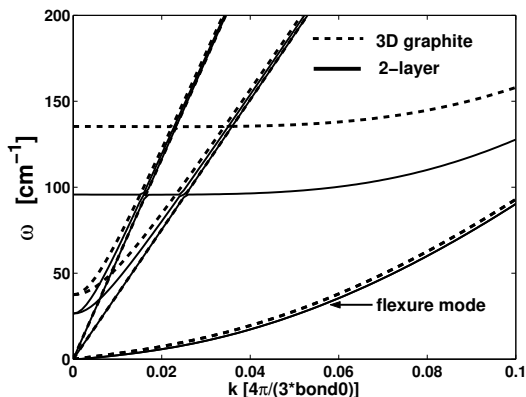


FIG. 5: The enlarged figure for the low-frequency region, where the significant difference between 3D graphite and the 2-layer graphene lies in.

the 3D graphite which are related only to the inter-layer interactions, yet independent of the intra-layer interactions. The inter-layer force constants are then fitted as $\hat{k}_l = 0.96Nm^{-1}$, $\hat{k}_{sl} = 0.73Nm^{-1}$, and $\hat{k}_{tw} = 0.8Nm^{-1}$. As shown in Table I, the fitted error is kept less than 7%. Base on the above fitted vibrational potential energy with eight terms, we calculate the dispersion curves for the graphite as shown in Fig. 2 (a). As illustrated in Fig. 3, and 4, our theoretical calculations meet the

experimental results not only in the low frequency¹¹ but also in the high frequency regions¹². The excellent consistency with the experimental data shows that our model and parameters are reasonable and applicable.

As an example of the ENSGL's, we consider the phonon dispersion for the 2-layer graphene. The calculated phonon dispersion curves along high-symmetry axes are displayed in Fig 2 (b). The most significant difference between the 2-layer graphene and the 3D graphite lies in the low-frequency region around the Γ point which is highlighted in Fig 5. The frequencies of the low-frequency optical modes in the 2-layer graphene are much smaller than its counterpart in the 3D graphite while the high optical modes have almost the same frequency values as those in the 3D graphite. The frequencies of the Raman and IR active modes are shown in the third line of Tables. II among which the two A_{1g} modes have the frequency value $\omega_1 = 95.72\text{cm}^{-1}$ and $\omega_2 = 867.07\text{cm}^{-1}$. In fact, ω_1 and ω_2 modes are the above mentioned NA_{1g} modes of the ENSGL's specified to $N = 2$.

We further calculate the phonon dispersion for the 3-layer graphene as the representative of the ONSGL's. In the fourth line of Tables. II, the Raman and Ir active modes are shown. There is an interesting phenomenon in the vibrational displacement for the modes at Γ point due to the σ_h symmetry operation ($\in D_{3h}$). The atoms in the middle layer keep quiescent when the outer two layers move out of phase. However, if the outer two layers move in phase, the middle layer atoms can oscillate along the same direction with a proper phase and amplitude. The former belongs to the irreducible representation A_1' and the latter is Ir active corresponding to A_2'' which involves exactly the ω_1 mode mentioned above with calculated frequency as 117.23cm^{-1} .

The lattice dynamical calculation for the frequencies of the ω_1 mode in 2- and 3-layered graphene provides an quantitative estimation and might inspire considerably the experimental interest to the ω_1 mode.

As a final remark, we address that our symmetry analysis for NSGL's is not only meaningful for its lattice dynamics, but also provides a fundamental point of view in investigating the various properties of the NSGL's.

* Electronic address: jwjiang@itp.ac.cn

¹ K. S. Novoselov et al., *Science* **306**, 666 (2004); C. Berger et al., *J. Phys. Chem. B* **108**, 19 912 (2004).

² B. Partoens and F. M. Peeters, *Phys. Rev. B* **74**, 075404 (2006); *Phys. Rev. B* **75**, 193402 (2007).

³ T. Aizawa, R. Souda, S. Otani, Y. Ishizawa, and C. Oshima, *Phys. Rev. B* **42**, 11469 (1990); **43**, 12060(E) (1991).

⁴ R. Saito, G. Dresselhaus, and M.S. Dresselhaus, *Physical Properties of Carbon Nanotubes* (Imperial College Press, 1998).

⁵ L. Brillson, E. Burskin, A. A. Maradudin, and T. Stark, *The Physics of Semimetals and Narrow-Gap Semiconductors*, Ed. D. L. Carter and R. T. Bate, (Pergamon Press,

London/Oxford 1971).

⁶ J. P. Elliott and P. G. Dawber, *Symmetry in Physics, Vol. 1*, (Macmillan Press, Ltd., 1979).

⁷ Eyring, Walter, and Kimball, *Quantum Chemistry*, John Wiley and Sons, (Inc., New York, 1940).

⁸ K. K. Mani and R. Ramani, *Phys. Status Solidi B* **61**, 659 (1974).

⁹ J. W. Jiang, H. Tang, B. S. Wang, and Z. B. Su, *Phys. Rev. B* **73**, 235434 (2006).

¹⁰ Jin-Wu Jiang, Hui Tang, Bing-Shen Wang and Zhao-Bin Su, arXiv:cond-mat/0610792.

¹¹ R. Nicklow et al., *Phys. Rev. B* **5**, 4951 (1972).

¹² J. Maultzsch et al., *Phys. Rev. Lett.* **92**, 075501 (2004).